International Journal for Modern Trends in Science and Technology, 9(05): 761-769, 2023

ISSN: 2455-3778 online
DOI: https://doi.org/10.46501/IJMTST0905131
Available online at: http://www.ijmtst.com/vol9issue05.html

Adaptive Control Based a Novel High-Gain DC-DC Boost Converter Solar Micro Grid Connected BLDC Water Pumping System

S. Chamundeswari[1] | Dr. J. Srinu Naick[2]

[1]Department of Electrical and Electronic Engineering, Chadalawada Ramanamma Engineering College, Tirupati, Andhra Pradesh, India.
[2]Department of Electrical and Electronic Engineering, Chadalawada Ramanamma Engineering College, Tirupati, Andhra Pradesh, India.

To Cite this Article
S. Chamundeswari and Dr. J. Srinu Naick. Adaptive Control Based a Novel High-Gain DC-DC Boost Converter Solar Micro Grid Connected BLDC Water Pumping System. International Journal for Modern Trends in Science and Technology 2023, 9(05), pp. 761-769. https://doi.org/10.46501/IJMTST0905131

Article Info
Received: 12 April 2023; Accepted: 02 May 2023; Published: 22 May 2023.

ABSTRACT

A novel high-gain DC-DC boost converter is demonstrated. A BLDC water pump that is connected to a solar micro grid is recommended. This work proposes a high DC voltage gain converter that uses far less components than existing high voltage gain DC-DC converters recently demonstrated in the literature. The proposed converter achieves significant voltage gain with a minimum of components using just one power switch, two inductors, two capacitors, and three diodes. This research demonstrates bidirectional control of power flow for a grid-connected solar photovoltaic (PV) water pump. There is an adaptive speed driver and a brushless DC (BLDC) motor in a permanent magnet motor and drive system. This allows the full capacity of a PV array and motor-pump to be utilized. It improves the dependability of the pumping system as well. The bidirectional flow of power between the grid and the DC bus of a voltage source inverter (VSI) that powers a brushless DC motor is regulated by a single-phase voltage source converter (VSC) employing a unit vector template (UVT) generation approach. Since the VSI operates at its fundamental frequency, switching loss is minimized. Maximum power point (MPP) functioning of a PV array, as determined by an ANFIS, is attained in this setup, as are power quality enhancements such power factor correction and a reduction in the grid's total harmonic distortion (THD). From a BLDC drive system mathematical model, a closed loop system is developed in this research using the adaptive-network-based fuzzy interference system (ANFIS). The BLDC motors driving systems ANFIS-based control is simulated using a nonlinear model in MATLAB/Simulink.

KEYWORDS: Maximum power point; Power quality; DC-DC converters; Voltage boosting methods; DC-DC converters; Brushless DC motors; Voltage source converters; Voltage source inverters.

1. INTRODUCTION

Renewable energy sources, such as solar panels, wind turbines, and biogas, will gradually replace traditional power plants and their associated fossil fuels. This will help lower global warming. Using renewable sources [1] at the same time is a bigger task because the power they make is of different types (AC or DC) and changes as the weather and environment change. Water pumps that run on nonrenewable fuels like oil and coal have a clear environmental disadvantage compared to solar photovoltaic technology, which can be deployed on a much grander scale. One way to meet the water demand is with a solar photovoltaic water pumping system that works on its own (SPVWPS). This method is getting a lot of praise for use in irrigation, in the home, and in industry automation. SPVWPS has a lot of benefits for pumping areas that don't have access to the national power grid, have an endless supply of solar energy, and don't have good transportation options. The research for this study was done in [1, 2]. Controlling the speed of a BLDC motor requires maintaining the DC connection voltage at its specified value, which varies with the amount of sunlight. The transport industry has also expanded in social and economic significance in the modern era [4, 5]. The electric motors in today's fully electric vehicles (FEVs) are powered by stacks of batteries or fuel cells that together generate a DC voltage of about 100 V [6-7], while the DC bus bar in FEVs operates at 400 V. To convert the relatively low DC voltage provided by the backup batteries into the much higher DC voltage required by the DC bus bar, a high-gain DC boost converter is required. In this study, a DC-DC boost converter is proposed as a potential answer to such issues, where a compact device with high voltage gain is required. There is a single power MOSFET, three diodes, two inductors, and two capacitors in the proposed converter. As a result, there are a lot less parts compared to other proposed designs for high-voltage gain DC-DC converters. The system depicted in achieves a high DC voltage gain via a cascade structure. In the first stage, a quadratic boost converter is used to enhance the voltage, and then a Cuk converter is used to smooth out the output. The current BLDC motor driven water pumps powered by a PV array only utilize energy from the sun while operating in a grid-isolated or stand-alone configuration. The most significant drawback of solar PV power is its intermittent nature. This reduces the reliability of water pumping systems. Bad weather makes it difficult to pump water, so the system doesn't benefit to its fullest extent when it's in use. Also, when there is no sunlight (at night), the water pumping device stops working. These problems need to be fixed in order to get a stable pumping system that uses PV. The use of battery-powered brushless DC (BLDC) motor drives has been tried before [8-9], but without success. The battery is charged while the sun is shining brightly and discharged when the sun is not out. This ensures that there is always enough water to go around. However, a PV-based water pumping system with added battery energy storage is not only more expensive but also more difficult to maintain [10, 11]. The typical lifespan of lead acid batteries is only a few years. The aforementioned shortcomings of battery storage have prompted the search for an alternative technological solution, which may be superior in every respect than batteries in the context of a dependable PV-powered water pumping system. These recently recognized technologies really link a PV generator set up to pump water to the mains power supply. No matter the time of day or night, it is crucial that the water flow remains constant and at full capacity. In [12], the author describes how a power distribution system in a grid-connected solar water pumping system chooses between using electricity from a PV array and power from the utility when the PV array isn't producing enough energy to run the pump. The DC bus shared by the PV array and the grid-connected inverter also connects to a water pump and a pump controller. Since there is no battery storage, the system's lifespan is increased while the cost of maintenance and production is decreased. This technique can be utilized in the DC bus bar of a fuel-cell vehicle, for example, where a massive voltage gain is required. High voltage gain, however, requires a significantly larger number of components. Despite only having a single power switch, the three inductors, four diodes, and four capacitors in [13] make for a more complex design. This makes it more difficult to employ. Much has been written and discussed about the structure and learning mechanisms of ANFIS (adaptive-network-based fuzzy inference system). The ANFIS is an adaptive-network-based fuzzy reasoning system. ANFIS 10 now has room for two input variables and one control output variable. The nonlinearity in the torque-balance equation is modelled in this study, and an ANFIS controller is developed to enhance the PMBLDC motor's transient response to torque disturbances.

- The BLDC motor-driven, solar-powered water pumping system is wired into the public power grid for redundancy.
- To guarantee the complete amount of water is given at all times, regardless of the weather, a

bidirectional power flow control is proposed.

- If the water pumping isn't necessary, the method as proposed allows the PV array's output to be sent back into the utility grid. This tool lets you use all of the installed resources to their full potential. Also, the system makes money by selling power to the utility company.
- The proposed water pumping system is constructed and regulated in such a way that it can continue to operate in the absence of grid power. The amount of water supplied is thus dependent on the amount of available sunshine.

2. CONFIGURATION OF PROPOSED SYSTEM

The Novel High-Gain DC-DC Boost Converter Solar Micro Grid Connected BLDC Water Pumping System is depicted in one possible setup in Figure 1. The system's water pump is powered by a brushless DC motor. A BLDC motor-pump is powered by a PV array via a high DC voltage gain boost converter and VSI. Electronic switching of the BLDC motor is handled by the VSI, while the boost converter performs ANFIS-based MPPT of the PV array using the InC algorithm. The nonlinearity in the torque-balance equation is accounted for in the closed-loop model of a permanent-magnet brushless DC (PMBLDC) motor, and an ANFIS controller is developed to enhance the transient response after torque disturbances. The DC bus used by VSI operates off of a single-phase power supply. Power can flow in either way through a voltage source converter (VSC) thanks to a DC bus capacitor. When the water pump is not in use, the PV system just contributes power to the grid. Even though a water pump may be necessary, supplying electricity to the grid is more important. To allow electricity to flow from the grid to the VSC and to regulate the amount of harmonic current entering the supply, an interface inductor is installed in the line. An RC ripple filter is used to reduce harmful harmonics in the power supply.

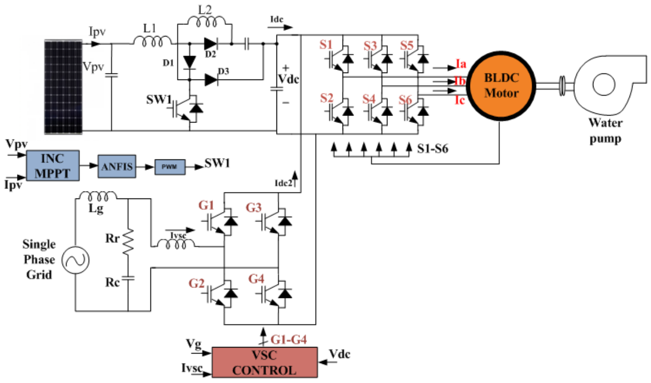

Fig. 1 schematic of the proposed PV array-based water pumping system with grid-interactive BLDC motor driving

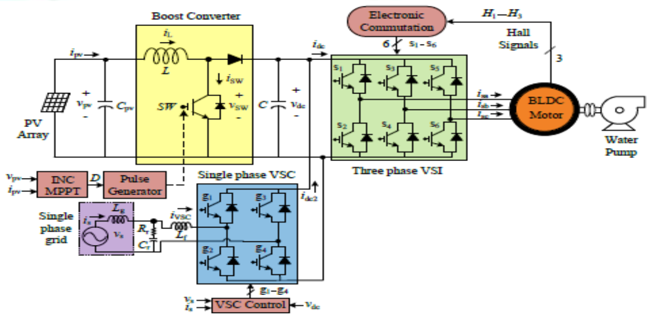

Fig.2 Existing method of a PV array-based water pumping system that works with the grid and uses a BLDC motor drive

3. SPEED CONTROL OF BLDCMOTOR

The performance of the speed driver for the BLDC drive that was made in Matlab has been looked at. A connectionist adaptable network-based fuzzy logic controller is made by combining the best parts of fuzzy logic and neural networks. The transient difference between the reaction and the set reference when the load torque changes is found to be negligibly small, and the ANFIS controller's time to settle is cut down in a good way. It is recommended for PMBLDC drive speed regulation due to its superior dynamic performance, precise tracking control, and solid steady-state qualities. First, the design for fuzzy logic control that is based on neural networks is explained. Different operating conditions are used to test how well the planned controller works

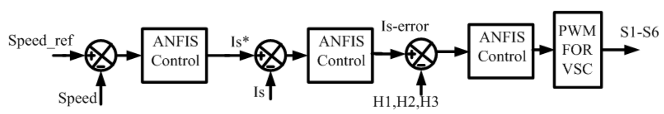

Fig. 2 Block diagram of the PWM controller for 3-level DCMLI.

4. BI-DIRECTIONAL POWER FLOW CONTROL

A PV generation that works with the grid makes it possible to build an effective water pumping system and use all of the available resources. As can be seen in Fig. 3, power can flow in either direction thanks to a UVT-based bidirectional power regulation. Since no advanced mathematical modelling or technique is required, this is the simplest approach. In order to synchronize with the grid's voltage and current, a single-phase PLL (Phase Locked Loop) is employed. Sinusoidal unit vector of supply voltage is produced at fundamental frequency. Altering the DC bus voltage, Vdc, results in a shift in the magnitude of the supply current's fundamental component, Isp. The voltage is controlled by a proportional-integral (PI) processor. A first-order low pass filter is used to the read vdc signal to eliminate the wave. Next, we check the filtered reading of Vdc against a target value, Vdc*. A significant portion of the supply current, Is*, can be calculated by multiplying Isp by sin. Gate pulses for VSC are generated by a current controller that compares the actual supply current (is) with the desired supply current (is*). The voltage regulator generates a positive I when it needs to draw power from the mains. That's why we tap into the grid for a current source that shares the same phase. Negative Isp is produced when PV arrays are used to power utilities, which results in an out-of-phase main current. Changing the direction of the current thereby alters the direction of the flow of electricity. Power quality on the utility grid is improved in terms of total harmonic distortion (THD) and power factor thanks to the employed method of regulation. Without access to the grid, adjusting the voltage on the DC bus is impossible. Despite the PV grid's sensitivity to weather, the water pump can still be powered independently.

5. CONVERTERS MODELLING

1. Designing for DC-DC High Gain Boost Converter

No matter the DC-DC converter's architecture, the energy storage component's design has a significant impact on the device's behavior and performance. The output DC voltage levels can be made more smooth and easier to regulate by limiting the ripple current of inductors and the ripple voltage of capacitors, respectively. The greatest current that could flow through an inductor should not be more than 10% of the maximum current that might flow through the inductor, as a rule of thumb. A capacitor's ripple voltage shouldn't be more than 10% of the maximum voltage that can develop up across it. Calculating the size of inductors and capacitors for a stable design that provides a constant current and a smooth level of voltage across the load is made easier with the help of these parameters. The calculated inductor and capacitor values for this proposed boost converter are depicted in fig. 4.

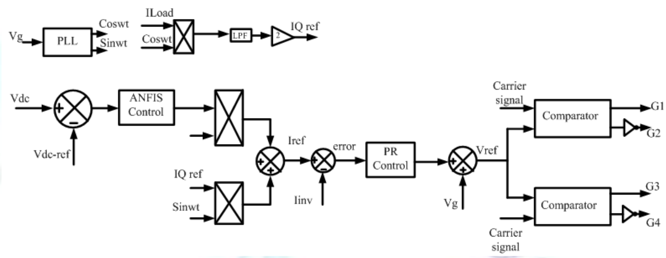

Fig. 3 ANFIS Control based bi-directional power flow control of VSC

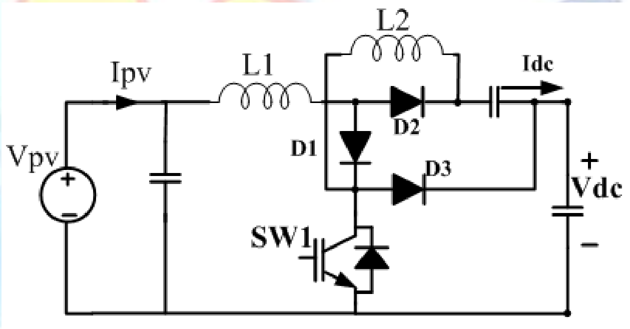

Fig. 4 a Novel High-Gain DC-DC Boost Converter

1.1 Design of Inductor L1

An inductor's voltage drop can be determined using

$$V_{in} = L\frac{dI_{L1}}{dt} \quad (1)$$

This leads to the following expression for the current in inductor L1:

$$\Delta I_{L1} = \frac{V_{in} \cdot D \cdot T}{L1} \quad (2)$$

A similar expression for the current in inductor L2 is

$$\Delta I_{L2} = \frac{V_{C1} \cdot D \cdot T}{L2} \quad (3)$$

Calculating the potential difference across capacitor C1:

$$V_{C1} \cdot D \cdot \frac{1}{L2 \cdot f_s} = V_{in}\left(\frac{D}{1-D}\right) \cdot \frac{1}{L2 \cdot f_s} \quad (4)$$

From (3),

$$\Delta I_{L2} = V_{C1} \cdot D \cdot \frac{1}{L2 \cdot f_s} \quad (5)$$

Comparing (4) and (5) gives

$$\Delta I_{L2} = V_{in} \cdot \frac{D}{1-D} \cdot \frac{1}{L2 \cdot f_s} \quad (6)$$

From (2), and in terms of Vout and fs

$$L1 = \frac{V_{out}\,(1-D)^2 \cdot D}{\Delta I_{L1} f_s} \qquad (7)$$

The smallest practicable value for L1 inductor is provided by the relation in (7). fs is the switching frequency of the power switch, Vout is the DC voltage output by the converter, and D is the duty-cycle. The ripple in the L1 inductor current is denoted by ΔI_L1.

1.2. Design of Inductor L2

From (6),

$$L2 = \frac{V_{in} \cdot D}{\Delta I_{L2} \cdot (1+D) \cdot f_s} \qquad (8)$$

For a given Vin and output voltage Vout, the minimum value of the L2 inductor required is given by (8), where I_L2 is the ripple current in the L2.

1.3. Design of Capacitor C1

The current via the series-connected L2 and C1 in Mode 0 is calculated as

$$I_{C1} = C1 \cdot \frac{\Delta V_{C1}}{\Delta t} \qquad (9)$$

In Mode 0, this equation looks like this:

$$C1 = \frac{I_0 \cdot D \cdot T}{\Delta V_{in}} \qquad (10)$$

using the relation $V_{C1} = V_{in} \cdot \left(\frac{1}{1-D}\right)$ (11)

$$\frac{\Delta V_{C1}}{\Delta V_{in}} = \frac{1}{1-D}$$

Hence (10) becomes

$$C1 = \frac{I_0 \cdot D}{\Delta V_{C1} \cdot (1-D) \cdot f_s} \qquad (12)$$

The minimal value of C1 that can be used with ΔV_c1 waves in the voltage across C1 is given by the relationship (12).

1.4. Design of Capacitor Co

The value of the current flowing through capacitor C2 is:

$$I_{Co} = Co \cdot \frac{dV_{out}}{dt} \qquad (13)$$

In Mode 0

$$Co = I_{Co} \cdot \frac{D}{\Delta V_{out} \cdot f_s} \qquad (14)$$

When the output voltage has ripples of ΔVOut t, the minimum value of the output capacitor is given by the equation (14). The converter's duty-cycle determines the maximum value of the output capacitor if the switching frequency, output voltage ripple, and output capacitor current remain constant. In order to produce the output capacitor, the converter must be operated at its maximum duty-cycle.

2. PROPOSED ANFIS BASED CONTROL

An adaptive network is a form of network that consists of nodes and dynamic links that connect the nodes, as suggested by the name. All or most of the nodes also exhibit adaptive behavior. This signifies that the learning rule specifies how the parameters of this node should be adjusted in order to minimize a specified error measure at each of its outputs.

Gradient descent and the chain rule provide the foundation of adaptive networks' primary method of learning. Fuzzy logic control (FLC) is a useful tool for dealing with uncertain, nonlinear, and complex systems. Learning, adapting, robustness, and speed are just few of the many impressive abilities of artificial neural networks (ANNs).

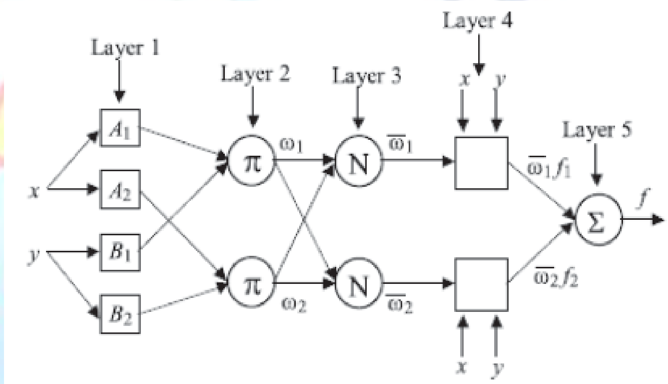

Figure. 5 Adaptive Neural Network

ANFIS combines the FLC and ANN to maximise the strengths of each. In operation, ANFIS, an adaptive network, is analogous to a fuzzy inference system. The PMBLDC drive's non-linearity and sensitivity to parameter fluctuations are both addressed by this control method. Here, ANFIS is adapted to work with a PMBLDC motor. In Fig.5, we have an example of an adaptive network, which is a multilayer feed forward network in which each node performs a specific function (node function) on incoming signals and a set of parameters related to this node. It's possible that the node function formula will vary from node to node. Consider a rule-based sugeno fuzzy system.

(i) f1 = p1 + q1 + r1 if (x, y) are elements of set A1 and set B1.

(ii)f2 = p2 x + q2y + r2 if x is A2 and y is B2.

For a given set of values for Ai and the integral of Bi, the output is computed as a weighted average if the rule fi ring strengths are w1 and w2.

$$f = \frac{w_1 f_1 + w_2 f_2}{w_1 + w_2} \quad (15)$$

Fuzzy sets Ai, Bi, i = 1,2 have membership functions A_i and B_i respectively.

Layer 1: The activation function of each layer 1 neuron "i" is parametric, making them all adaptable. It returns a function representing the membership level; the generalized bell shape function is an example $\mu(x) = \frac{1}{1+\left[\frac{x-c}{a}\right]^{2b}}$ (16)

Where the input set is [a, b, c]. The shape of a bell-shaped function changes as the values of the factors change.

Layer 2: To which [a, b, c] is the input data set. As the values of the components vary, the bell-shaped function takes on many forms.

$$w_i = \mu A_i(x)\mu B_i(y), \quad i = 1,2 \quad (17)$$

Layer 3: Each input is normalized by this layer. The result of the ith node is the ith input divided by the sum of the other inputs.

$$\bar{w}_i = \frac{w_i}{w_1 + w_2} \quad (18)$$

Layer 4: This layer's ith node output is proportional to the ANFIS input signals and the third layer's ith node output.

$$\bar{w}_i f_i = \bar{w}_i(p_i x + p_i y + r_i) \quad (19)$$

Layer 5: This layer adds up all the data that come in.

$$f = \bar{w}_1 f_1 + \bar{w}_2 f \quad (20)$$

6. SIMULATION RESULTS AND DISCUSSION

The results of the simulations in the MATLAB/Simulink platform are used to look at how the suggested system works in different ways. The water pump can be run only with a PV array, only with the grid, both with a PV array and with the grid, or not at all. For the demonstration of the suggested system, all of these possible operating conditions are taken into account. Start-up, dynamic, and steady-state processes are all tested on the system and its control. First, in this work, a model of a drive with a PI Speed driver is made and simulated. The model of the driving system, a collection of equations, has been discussed. Layer 1 of the ANFIS structure is taught utilizing the Matlab GUI tool box of ANFIS by inputting the speed error and the change in speed error from the PI controller. The resulting membership functions for speed inaccuracy and velocity variation are displayed in Figure 8.

A. Starting and Steady State Performance

The main goals of these performance studies are to show how a BLDC motor starts up smoothly and how a motor-pump works in a steady state under different working conditions.

a. Starting and Steady State Performance

(1) When the pump feeding the PV array is switched to a pump feeding both the PV array and the grid, and (2) the pump feeding the grid is switched to a pump feeding both the PV array and the grid, the WPS's beginning performance is demonstrated. The initial function is shown to be smooth across all inputs.

1. Change from a pump that fed the PV array to a pump that fed both the PV array and the grid:

Since the PV array and the grid are both capable of powering the pump at full capacity, it is assumed that this is the case. The water pump requires more power than the PV array can provide, so electricity from the grid is also required. This is depicted in Fig. 6. With 400 V applied to the DC bus, the motor can reach speeds of 3000 rpm.

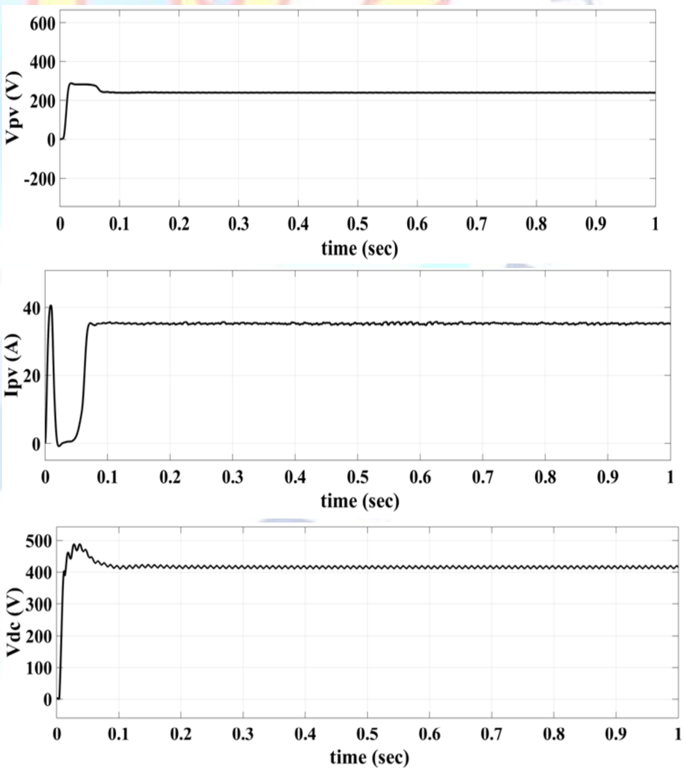

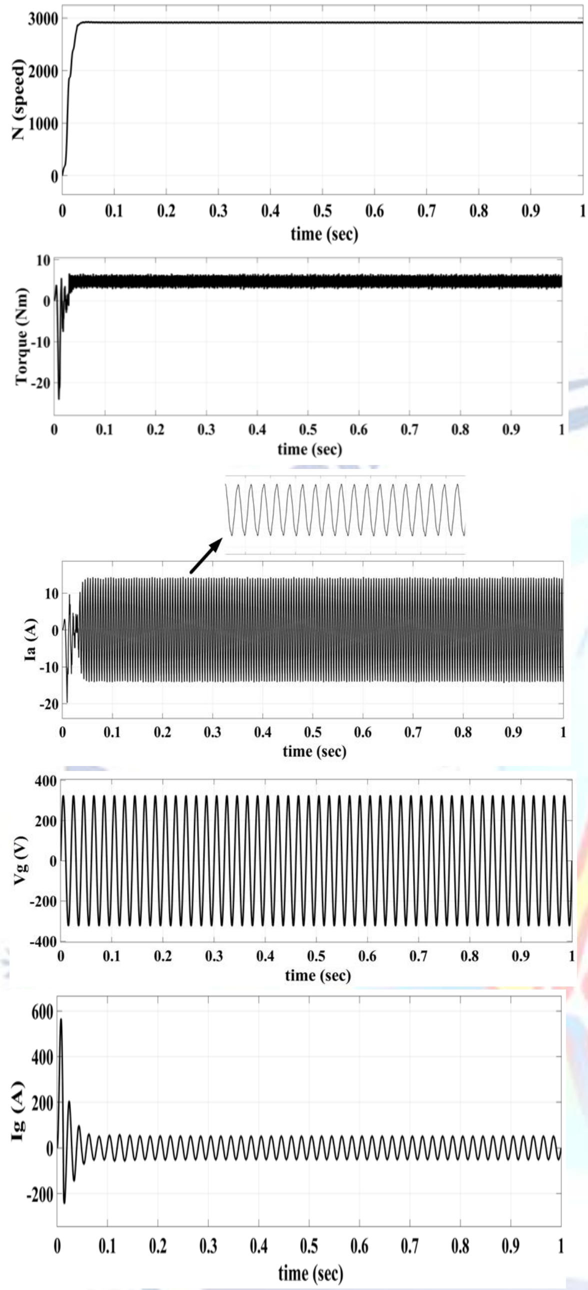

Fig. 6 The interplay between a photovoltaic (PV) array, the power grid, and a brushless DC (BLDC) motor-pump when the pump is switched from being fed by the PV array to being fed by both the PV array and the grid.

B. Performance on the Move A dynamic situation is one in which the weather changes quickly or the direction of the power flow needs to change quickly. The suggested system is tested to make sure it works well with the dynamics in mind.

1) Change from a pump feeding the grid to a PV array feeding the grid:

In the absence of power from the PV array, the utility grid is assumed to kick in and power the water pump first in this analysis. The mode of operation shifts swiftly when one considers the possibility of not needing to pump water and of having power available from a PV array. So, a PV array is the target for powering the service. Figure 7 depicts the results obtained in this dynamic setting. The machine's operation modifies itself every 0.5 s. Figure 7 displays the PV array, power grid, and BLDC motor pump indices. The DC bus voltage is maintained at 400 V, as indicated in Fig. 6. As can be seen in Fig. 7, the motor-pump slows to a stop after about a minute and a half.

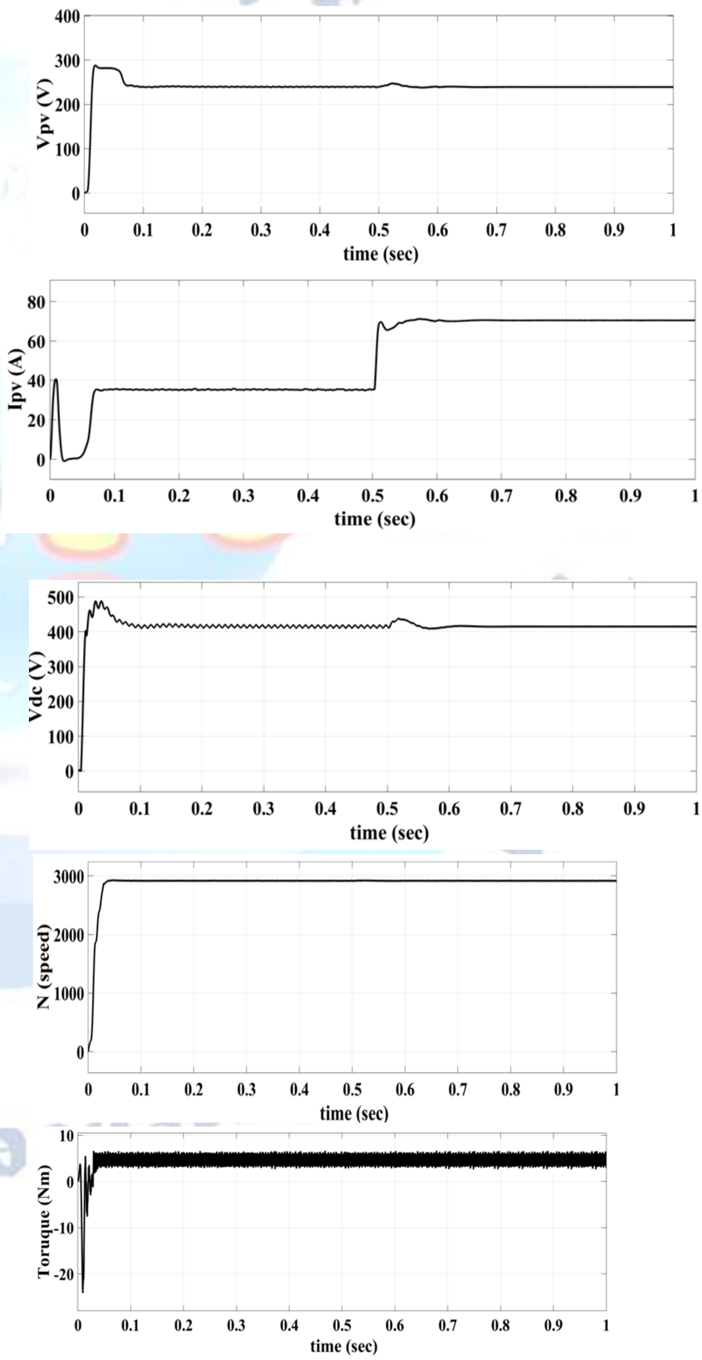

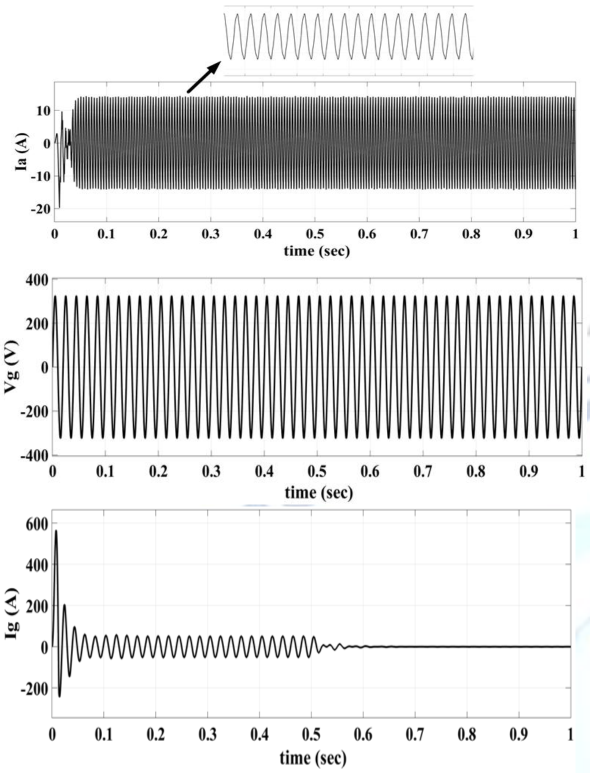

Fig. 7 The dynamic response of the PV array, utility grid, and BLDC motor when grid power is cut off to the pump and vice versa.

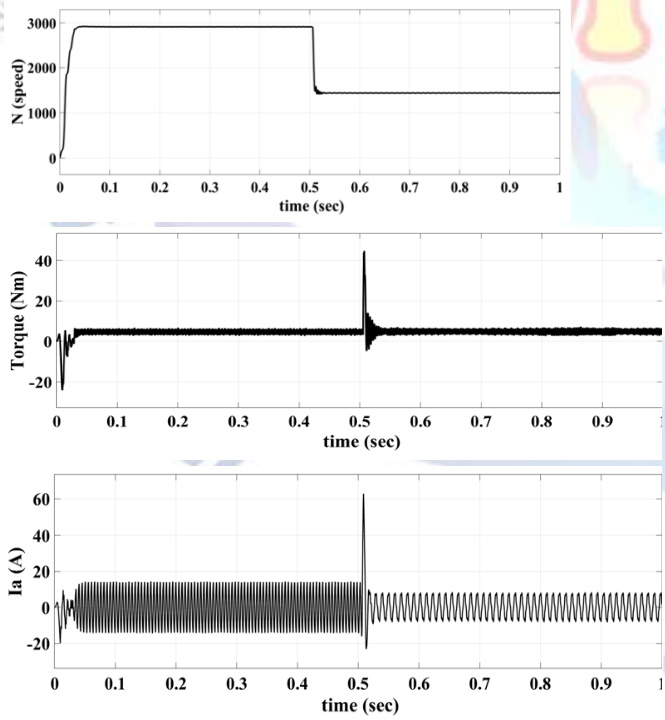

Fig. 8 The dynamic reaction of a BLDC motor during a switch from a grid-fed pump to a grid-fed PV array

7. CONCLUSIONS

This research proposes a novel high-gain DC-DC boost converter-equipped BLDC solar micro grid-connected water pumping system. This work demonstrates a novel DC-DC boost converter that, compared to recently introduce high DC voltage gain boost converters, requires fewer components. The efficiency, voltage stresses, and DC voltage gain of the proposed boost converter were all simulated. The objective was to find the most effective way to model the system and develop an MPPT technique that did not rely on the size of the steps. Based on the findings, an ANFIS-based MPPT is a viable option for developing grid-connected water pumping systems that use BLDC motors regardless of step size. Good transient and steady-state performance of the system has been seen across a broad irradiance range. Fuzzy logic and neural networks' strengths are combined to create a connectionist adaptable network-based fuzzy logic controller. The ANFIS controller's time to settle is improved, and the transient discrepancy between the reaction and the set reference when the load torque changes is determined to be modest. With VSC's bidirectional power flow control, all available resources may be utilized, and water can be pumped at maximum capacity regardless of external factors. The speed of a BLDC motor-pump can be regulated without the need for any current-sensing components. The whole system efficiency has increased thanks to the fundamental frequency switching of VSI, which has reduced switching losses. The proposed solution provides not only a dependable means of pumping water, but also an opportunity to earn money by selling energy to the utility company at times when water pumping is unnecessary.

Conflict of interest statement

Authors declare that they do not have any conflict of interest.

References

[1] V. K. A. Shankar, S. Umashankar, S. Padmanaban, M. S. Bhaskar, V. K. Ramachandaramurthy and V. Fedak, “Comparative study of photovoltaic based power converter topologies for pumping applicat ions,”IEEE Conference on Energy Conversion (CENCON),Kuala Lumpur, Malaysia, pp. 174-179, 2017.

[2] Rajan Kumar and Bhim Singh , "BLDC motor driven water pump fed by solar photovoltaic array using boost converter," in Annual IEEE India Conf. (INDICON), New Delhi, 2015.

[3] Bhim Singh and Ranjan Kumar, "Solar PV Array Fed Brushless DC Motor Driven water pump," in IEEE 6th International Conference on Power Systems (ICPS), New Delhi, 2016.

[4] Khaligh, A.; Li, Z. Battery, Ultracapacitor, Fuel Cell, and Hybrid Energy Storage Systems for Electric, Hybrid Electric, Fuel Cell, and Plug-In Hybrid Electric Vehicles: State of the Art. IEEE Trans. Veh. Technol. 2010, 59, 2806–2814.

[5] Lai, C.-M.; Cheng, Y.-H.; Hsieh, M.-H.; Lin, Y.-C. Development of a Bidirectional DC/DC Converter with Dual-Battery Energy Storage for Hybrid Electric Vehicle System. IEEE Trans. Veh. Technol. 2017, 67, 1036–1052.

[6] Forouzesh, M.; Siwakoti, Y.P.; Gorji, S.A.; Blaabjerg, F.; Lehman, B. Step-Up DC–DC Converters: A Comprehensive Review of Voltage-Boosting Techniques, Topologies, and Applications. IEEE Trans. Power Electron. 2017, 32, 9143–9178.

[7] Pires, V.F.; Cordeiro, A.; Foito, D.; Silva, J.F. High Step-Up DC-DC Converter for Fuel Cell Vehicles Based on Merged Quadratic Boost-Cuk. IEEE Trans. Veh. Technol. 2019, 68, 7521–7530.

[8] K. Rahrah, D. Rekioua, T. Rekioua and S. Bacha, "Photovoltaic pumping system in Bejaia climate with battery storage," International Journal of Hydrogen Energy, vol. 40, no. 39, pp. 13665-13675, 19 October 2015.

[9] Abla Khiareddine, Chokri Ben Salah and Mohamed Faouzi Mimouni, "Power management of a photovoltaic/battery pumping system in agricultural experiment station," Solar Energy, vol. 112, pp. 319-338, February 2015.

[10] J. H. Ugale and M. S. Panse, "Single phase AC drive for isolated solar photovoltaic water pumping system," International Conference on Green Computing and Internet of Things (ICGCIoT), Noida, 2015, pp. 1285-1287.

[11] A. Boussaibo, M. Kamta, J. Kayem, D. Toader, S. Haragus and A. Maghet, "Characterization of photovoltaic pumping system model without battery storage by MATLAB/Simulink," 9th International Symposium on Advanced Topics in Electrical Engineering (ATEE), Bucharest, 2015, pp. 774-780.

[12] Huang, "Photovoltaic Water Pumping and Residual Electricity Grid- Connected System," Chinese Patent CN 204131142 U, Jan. 28, 2015.

[13] J.-S. Roger Jang and C.-T. Sun, "Neuro-Fuzzy Modeling and Control", Proceedings of the IEEE, vol.83, no.3, pp. 378-406, March 1995.